



Research Article

<https://doi.org/10.1631/jzus.B2500747>

Integrative analytical and statistical framework for optimization of multiplex qPCR detection of *TGFBI* mutations in refractive surgery candidates

Yunfeng GU¹, Liping MAO¹, Xiaoling LI², Kangxuan SUN³, Qiuruo JIANG¹, Wenhui WU², Yangyang SHEN¹, Shihao CHEN¹✉, Meiqin ZHENG¹✉, Yi XU¹✉

¹National Clinical Research Center for Ocular Diseases, Eye Hospital, Wenzhou Medical University, Wenzhou 325027, China

²Institute of PSI Genomics, Wenzhou Global Eye & Vision Innovation Center, Wenzhou, 325024, China

³Key Laboratory of Laboratory Medicine, Ministry of Education, School of Laboratory Medicine and Life Sciences, Wenzhou Medical University, Wenzhou 325035, China

Abstract: Refractive surgery can unmask or accelerate transforming growth factor beta-induced (*TGFBI*)-related corneal dystrophies that are undetectable by routine slit-lamp examination, creating a clear need for a rapid, standardized, preoperative genetic screening. We developed a multiplex, allele-specific quantitative polymerase chain reaction (qPCR) panel targeting five high-frequency *TGFBI* hotspots (R124C/L/H, R555W/Q) and built a statistics-driven analytical framework to optimize assay decisions. Receiver-operating-characteristic (ROC) analysis defined locus-specific cycle threshold (Ct) cutoffs that were harmonized to a single decision threshold (Ct=36) to simplify deployment. Analytical sensitivity was established by Probit modeling of serial two-fold dilutions, and confirmed by ≥ 20 replicates per level. In a 158-sample validation set (38 mutation-positive; 120 negative), qPCR agreed perfectly with Sanger sequencing (Cohen's Kappa coefficient (κ)=1.0). Probit analysis yielded locus-specific limit-of-detection (LoD) values ranging from 0.035–0.20 ng μL^{-1} ; at 0.20 ng μL^{-1} the detection rate was over 95%. Repeatability and intermediate precision were high (Ct coefficient of variation (CV) 0.34–1.21%). No cross-reactivity was observed against non-target *TGFBI* variants or other ophthalmic genes, and interference from blood, oral flora/rinse, or toothpaste produced small, bounded shifts ($\approx -7.8\%$ to $+2.8\%$). Calibration with serial dilutions demonstrated linear Ct–log(copy) relationships suitable for routine quality control. Prospective screening of 10,055 refractive surgery candidates identified six *TGFBI* carriers (0.06%) harboring R124H (including one homozygote), R124L, R124C, or R555W mutations, all confirmed by Sanger sequencing. This study established a clinically applicable, statistically optimized multiplex qPCR platform that integrates ROC-derived cutoffs and Probit-defined LoD with rigorous evaluations of precision, specificity and robustness, enabling large-scale population implementation. Positive screening results guide clinical decision-making through a standardized post-screening workflow, and the targeted hotspot screening strategy serves as a cost-effective first-tier high-throughput approach for preoperative risk assessment. The framework provides a transparent, reproducible path to standardize preoperative *TGFBI* screening and reduce iatrogenic risk in refractive surgery candidates.

Key words: Multiplex quantitative polymerase chain reaction (qPCR); Analytical and statistical validation; Preoperative transforming growth factor beta-induced (*TGFBI*) mutation screening

✉ Yi XU, xy@eye.ac.cn

Meiqin ZHENG, zmq@eye.ac.cn

Shihao CHEN, chenle@rocketmail.com

✉ Yi Xu, <https://orcid.org/0009-0003-5409-7098>

Meiqin ZHENG, <https://orcid.org/0000-0003-3253-4480>

Shihao CHEN, <https://orcid.org/0000-0001-7646-8003>

Yunfeng GU, <https://orcid.org/0009-0005-5549-3716>

Received Nov. 19, 2025; Revision accepted Mar. 24, 2026;
Crosschecked xxx. xx, 20xx; Published online xxx. xx, 20xx

1 Introduction

Inherited corneal dystrophies, particularly those caused by transforming growth factor beta-induced (*TGFBI*) mutations, pose significant diagnostic and surgical challenges (Weiss et al., 2024). These disorders are often bilateral, progressive, and clinically heterogeneous, with certain genotypes—such as R124C/L/H and R555W/Q—representing over 90% of epithelial-stromal dystrophy cases in East Asian populations (Song et al., 2017; Cho et al., 2025). This high prevalence of the five hotspot mutations in East Asian populations is the core rationale for their selection as the assay targets in this study. In refractive surgery candidates, the subclinical presence of such mutations can precipitate corneal opacification following procedures like LASIK or PRK, leading to irreversible visual impairment (Stenson et al., 2020). Current slit-lamp-based screening methods lack the sensitivity to detect asymptomatic carriers, particularly in younger patients, creating an urgent clinical demand for rapid, quantitative, and standardized genetic testing before surgery (Chao-Shern et al., 2019; Li et al., 2021).

Although Sanger sequencing remains the clinical reference method for *TGFBI* genotyping, its long turnaround time and relatively high cost limit its application for large-scale presurgical screening (Han et al., 2016; Hieda et al., 2023). The integration of real-time quantitative polymerase chain reaction (qPCR) with statistical validation offers a compelling solution, enabling both rapid detection and rigorous analytical standardization (Bostan and Randleman, 2024). Here, we designed a multiplex allele-specific qPCR platform targeting five recurrent *TGFBI* hotspots and coupled it with statistical optimization tools—including receiver operating characteristic (ROC) curve analysis for threshold calibration and Probit modeling for limit-of-detection (LoD) estimation (Kwak et al., 2021). This dual analytical–statistical validation ensures the assay’s reproducibility, sensitivity, and clinical reliability, fulfilling the methodological rigor expected in analytical science (Jiang and Zhang, 2021).

A key strength of this work lies in its scale: over 10,000 preoperative samples were collected prospectively, yielding a robust and demographically representative dataset that enables objective performance evaluation in situations with real-world clinical variability (Rocha-De-Lossada et al., 2021). Such large-scale empirical validation bridges the gap between research and clinical utility, demonstrating the feasibility of standardized molecular diagnostics in routine surgical workflows. Statistical validation metrics—limit of blank (LoB), LoD, limit of quantification (LoQ), and ROC-derived cutoffs—were not merely descriptive but functioned as optimization levers, quantitatively refining assay performance (Munier et al., 1997; Song et al., 2023).

It is important to note that a negative result for the targeted hotspot mutations does not exclude the presence of rare or atypical pathogenic variants. Sanger sequencing is recommended for individuals with suspicious clinical phenotypes, positive family history, or abnormal imaging findings despite a negative qPCR screen, to address residual genetic risk. Ultimately, this study establishes an evidence-based, statistics-optimized workflow for genetic risk screening in refractive surgery candidates. By uniting molecular diagnostics with population-scale statistical evaluation, it provides an objective, reproducible framework to minimize postoperative complications, elevate preoperative safety standards, and offer a scientific foundation for future clinical laboratory guidelines (Fig. 1).

2 Materials and methods

2.1 Clinical samples and study design

Buccal swab samples were collected from the Eye Hospital of Wenzhou Medical University. To establish and validate the qPCR assay, we obtained swab samples from the Department of Cornea (Valasek and Repa, 2005). Preoperative genetic testing was conducted via swab sampling of 10,055 candidates for corneal laser surgery who were evaluated at the Department of Refractive Surgery between May 24, 2021, and December 31, 2024. This study adhered to the principles of the Declaration of Helsinki. Ethics approval was obtained from the Institutional Review Board, and written informed consent was obtained from all participants prior to genetic testing.

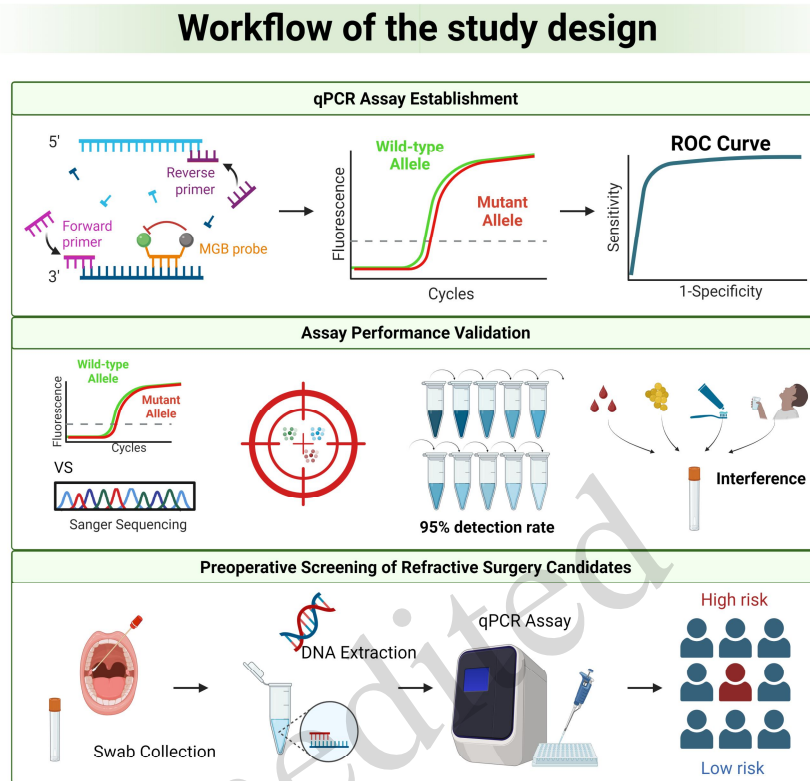


Fig. 1 Schematic overview of the workflow for multiplex allele-specific quantitative polymerase chain reaction (qPCR) screening of transforming growth factor beta-induced (*TGFB1*)- hotspot mutations, including buccal swab collection, genomic deoxyriboNucleic acid (DNA) extraction, qPCR targeted amplification, and result interpretation. ROC : receiver-operating-characteristic; VS: versus

2.2 Sample collection and genomic DNA extraction

Buccal specimens were collected using sterile nylon-flocked swabs and immediately transferred to collection tubes prefilled with a stabilizing agent (Skonier et al., 1992). DNA was extracted using the MagPure Tissue DNA Kit according to the manufacturer's protocol. DNA concentration and purity were assessed spectrophotometrically, and extracts were diluted to the intended working range for qPCR assays.

2.3 Design of multiplex allele-specific qPCR assays

Four allele-specific qPCR reactions were established to detect five hotspot mutations in *TGFB1*: c.370C>T, c.371G>A and c.371G>T, c.1663C>T, c.1664G>A.

Primer-probe sets (Supplementary, Table S1) were designed using conserved flanking regions and MGB-modified hydrolysis probes, each labeled with distinct fluorophores to differentiate wild-type and mutant alleles (Liskova et al., 2025). Amplicon lengths were kept between 85–100 bp to ensure high amplification efficiency. qPCR reactions (25 μ L) comprised 1 \times master mix, 300 nmol/L primers, 200 nmol/L probes, and 20–50 ng template DNA. Amplification was performed on an ABI 7500 Real-Time PCR System: 95 $^{\circ}$ C for 5 min; 40 cycles of 95 $^{\circ}$ C for 10 s and 65 $^{\circ}$ C for 40 s. Fluorescence was acquired at the annealing/extension step.

2.4 Analytical sensitivity: ROC-based Ct threshold calibration

To establish diagnostic thresholds, Ct distributions were obtained from: 30 wild-type samples, 10

heterozygotes, and ten-point serial dilutions of two homozygous mutation samples (10^0 – 10^{-3} ng/ μ L).

For each locus, we generated ROC curves by plotting sensitivity versus $1 - \text{specificity}$. Ct cutoffs maximizing the Youden index ($J = \text{sensitivity} + \text{specificity} - 1$) were selected (Holden et al., 2016). Since all loci showed highly similar discrimination performance, a unified cut-off of Ct = 36 was adopted for operational simplicity.

2.5 Limit-of-detection (LoD) determination via probit modeling

To quantify analytical sensitivity, LoD was estimated using two-fold serial dilutions of heterozygous genomic DNA (0.8–0.00625 ng/ μ L; $n = 5$ replicates per level). Detection rates across concentrations were modeled by a Probit regression, yielding the concentration corresponding to 95% detection probability (Gao et al., 2021).

LoD values (0.035–0.20 ng/ μ L across loci) were independently validated by testing 20 replicates at each concentration (0.4, 0.2, and 0.1 ng/ μ L). The lowest concentration with $\geq 95\%$ detection consistency was defined as the empirical LoD.

2.6 Precision and reproducibility studies

Assay precision was evaluated at low and high template concentrations. Intra-day precision: eight replicates per allele, evaluated on a single day. Inter-day precision: repeated across three non-consecutive days. Operator reproducibility: experiments performed by three independent technologists (Zhang and Song, 2023). Precision was expressed as cycle-threshold coefficient of variation (Ct CV%), with acceptable analytical reproducibility defined as $CV \leq 2\%$.

2.7 Specificity and cross-reactivity evaluation

Specificity was assessed using genomic DNA containing: non-target *TGFBI* variants, mutations in other ocular disease genes (e.g., *NMNAT1*, *EYS*, and *ABCA4*). Assays were considered specific when non-target templates produced no amplification (Ct ≥ 40) in mutant channels.

2.8 Interference testing

To assess robustness in a clinically realistic matrix, buccal DNA was spiked with: 5% venous blood, 300 colony-forming unit per milliliter (CFU/mL) *Staphylococcus aureus*, 5% mouthwash, 1 g/L toothpaste. Interference was defined as percent deviation of Ct values relative to non-spiked controls. Acceptable performance was predetermined as $< \pm 10\%$ Ct shift.

2.9 Standard curve construction and amplification efficiency

Serial dilutions of homozygous reference DNA (10^6 – 10^1 copies/reaction) were used to generate standard curves for each allele. Slope, coefficient of determination (R^2), and amplification efficiency were computed from Ct versus $\log(\text{copies})$ regression.

Efficiencies ranging between 90–110% and $R^2 \geq 0.98$ were considered analytically acceptable.

2.10 Sanger sequencing confirmation

For all qPCR-positive samples and 120 randomly selected negatives, bidirectional Sanger sequencing was performed (Wang et al., 2020). PCR products were purified and sequenced using ABI 3730 instruments. Chromatograms were manually reviewed to confirm allele calls.

2.11 Large-scale preoperative screening

All 10,055 participants were screened using the optimized qPCR assay. Individuals with Ct < 36 in any mutant channel were classified as mutation carriers. Positive cases were reviewed by corneal specialists and confirmed with Sanger sequencing. Demographic distribution and mutation frequency were summarized

descriptively.

A standardized post-screening clinical workflow was implemented for qPCR-positive individuals: (1) qPCR-positive results were confirmed by bidirectional Sanger sequencing; (2) screen-positive individuals were referred to corneal specialists for comprehensive clinical evaluation and genetic counseling; (3) treating clinicians determined surgical planning decisions (cancelling surgery, or modifying the surgical approach) based on the combined genetic and clinical findings.

2.12 Statistical analysis

Analytical performance metrics (sensitivity, specificity, Area Under Curve(AUC), LoD, and CV) were computed using MedCalc and GraphPad Prism. Continuous variables were reported as means \pm SD. Categorical variables were summarized as proportions with 95% confidence intervals. All statistical tests were two-sided, with $p < 0.05$ considered significant.

3 Results

3.1 Establishment of qPCR assay for *TGFBI* hotspot mutations

Four *TGFBI* hotspot mutations located in exons 4 and 12 were selected as assay targets (Fig. 2a). Custom-designed primer–probe sets (Table S1) were used to establish four locus-specific qPCR assays covering five clinically relevant variants: c.370C>T, c.371G>A, c.371G>T, c.1663C>T, and c.1664G>A. Among them, the c.371 assay enabled simultaneous discrimination of both c.371G>A and c.371G>T, while the remaining loci detected single-base substitutions individually. The AUC values of the ROC curves for all detection loci were 1.000 (95%CI: 1.000-1.000).

The assay was first evaluated using wild-type, heterozygous, and homozygous clinical samples, alongside recombinant plasmids and negative controls including genomic DNA from common oral bacteria and nuclease-free water. As shown in Fig. 2b–2e, wild-type samples produced only wild-type amplification curves, homozygous mutants yielded only mutant curves, and heterozygous specimens showed dual-signal amplification. No amplification was observed in any negative controls, confirming assay specificity at the qualitative level.

To determine the decision cutoff, we tested a panel of 30 wild-type, 10 heterozygous, and one homozygous sample for each locus across ten serial concentrations (Supplementary, Fig. S1). ROC curve analysis (Fig. 2f) yielded locus-specific Ct thresholds: c.370 (35.85/35.30), c.371 (35.71/34.76/35.24 for G/A/T), c.1663 (35.47/35.46), and c.1664 (36.12/35.62). To streamline interpretation and assay deployment, a unified cutoff of Ct = 36 was adopted for all targets.

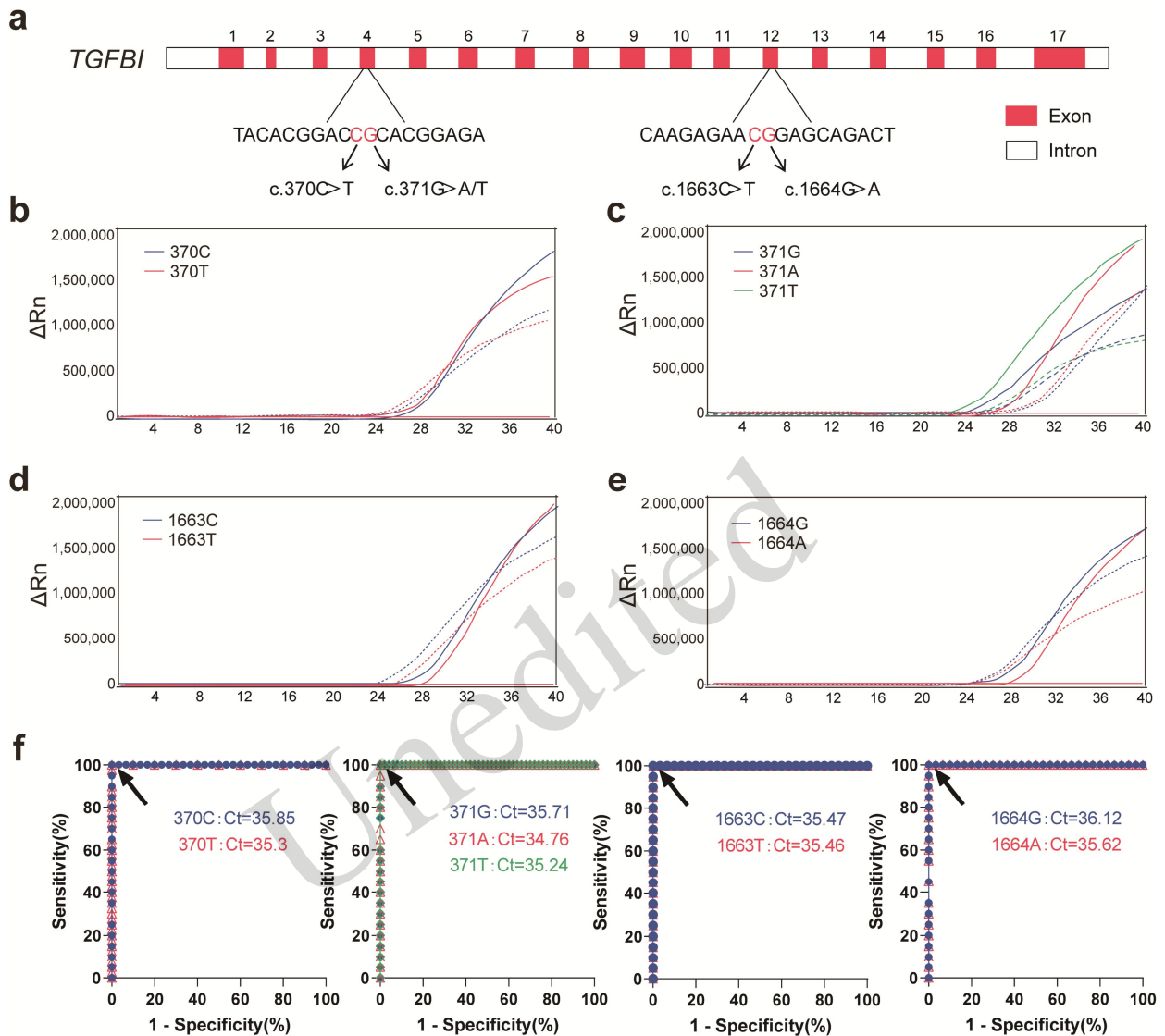


Fig. 2 Allele-specific quantitative polymerase chain reaction (qPCR) performance for the four transforming growth factor beta-induced (*TGFBI*) loci, showing distinct amplification patterns for wild-type and mutant alleles and ROC-derived Ct thresholds supporting accurate discrimination across all targeted hotspot mutations. (a) Genomic locations of the five hotspot mutation sites in the *TGFBI* gene. (b-e) Representative genotyping results for the loci c.370, c.371, c.1663, and c.1664 from clinical samples and recombinant plasmids. Wild-type alleles are indicated by blue lines, homozygous mutations by red or green lines, and heterozygous mutations by dashed lines. (f) ROC curve analysis of the qPCR assay for each locus.

3.2 Performance validation of the *TGFBI* qPCR assay

To assess analytical accuracy, 158 clinical samples (38 mutation-positive and 120 wild-type) were tested. qPCR results demonstrated identical results with Sanger sequencing ($\kappa = 1.0$), confirming assay accuracy for all five target mutations (Table S2).

Analytical sensitivity was evaluated using four heterozygous samples — including one artificially generated 371GAT pool — subjected to a two-fold dilution series from 0.8 ng/ μ L across ten concentrations. Each dilution was tested in five replicates, and Probit modeling was applied to estimate the lower limit of detection (LLOD). As shown in Fig. 3a, LLOD values were 0.162/0.035 ng/ μ L (c.370 C/T), 0.200/0.178/0.162 ng/ μ L (c.371 G/A/T), 0.081/0.041 ng/ μ L (c.1663 C/T), and 0.200/0.081 ng/ μ L (c.1664 G/A). The overall LLOD was therefore defined as 0.2 (95%CI: 0.182-0.231) ng/ μ L. To validate this cutoff, five heterozygous

samples were diluted to 0.4, 0.2, and 0.1 ng/ μ L and tested in 20 replicates (Supplementary, Table S3). A $\geq 95\%$ positive rate was consistently achieved at 0.2 ng/ μ L.

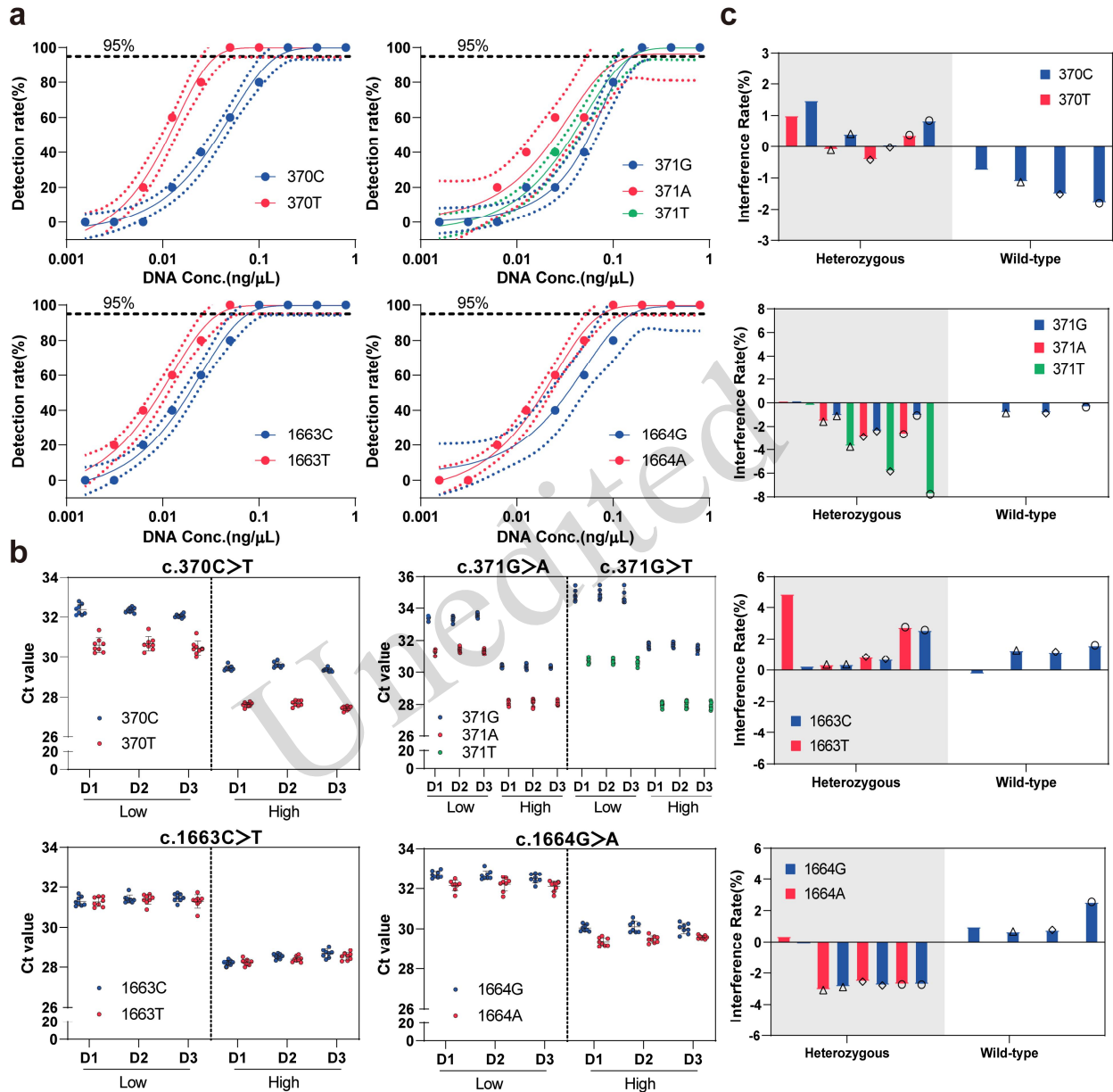


Fig. 3. Analytical sensitivity, precision, and robustness of the multiplex allele-specific quantitative polymerase chain reaction (qPCR) assay across all transforming growth factor beta-induced (*TGFBI*) hotspot loci. (a) Probit-modeled limits of detection using two-fold serial dilutions; (b) Intra- and inter-day reproducibility across operators and concentrations; (c) Interference testing with common contaminants in clinical samples.

To establish the limit of quantification (LoQ), heterozygous samples were tested across a broader concentration range (50–0.2 ng/ μ L). Linear regression of Ct versus log₁₀ concentration demonstrated high linearity, and LoQ was defined as the lowest concentration with Ct CV <5%. Corresponding slopes, amplification efficiencies, R² values, and LoQs for each locus are summarized in Table S4 and Fig. 2.

We examined reproducibility using heterozygous samples prepared at high and low concentrations for each locus. Samples were analyzed by different operators over three consecutive days, with eight replicates per day. As shown in Fig. 3b, intra- and inter-day Ct values displayed no statistically significant variation, and CVs

ranged from 0.34% to 1.21%, supporting stable assay performance.

Specificity was assessed using ten samples carrying alternative *TGFBI* mutations. Each hotspot variant was detected only by its corresponding assay, while samples with other *TGFBI* mutations produced negative results (Supplementary, Table S5). All eight samples harboring mutations in other ocular disease genes were also negative (Supplementary, Table S6), supporting high analytical specificity. Taken together, the specificity of the detection system was 100% (95%CI: 99.25%–100.00%).

To evaluate robustness, potential interference from venous blood, *Staphylococcus aureus*, mouthwash, and toothpaste was examined in both heterozygous and wild-type samples. Interference rates remained low across all conditions (Fig. 3c): –0.77% to 1.48% (5% blood), –3.75% to 1.29% (300 CFU/mL *S. aureus*), –5.85% to 0.84% (5% mouthwash), and –7.78% to 2.77% (1 g/L toothpaste), indicating strong assay tolerance to common contaminants.

3.3 Preoperative screening of refractive surgery candidates

The assay was administered to 10,055 individuals undergoing preoperative evaluation for corneal refractive surgery. Six individuals (0.06%) were identified as mutation carriers (Supplementary Table S7, Fig. 4a) but slit-lamp examination showed no obvious corneal abnormalities. The overall cohort consisted of 6,312 males (62.8%) and 3,743 females (37.2%), with a mean age of 22.57 ± 5.94 years.

Among mutation-positive individuals (four males and two females; mean age 22.67 ± 4.23 years), no significant differences in sex ($P = 1.00$) or age ($P = 0.91$) were observed compared with mutation-negative participants. Identified variants included two cases of c.371G>A (p.R124H), one of which was homozygous, as well as single cases of c.371G>T (p.R124L), c.370C>T (p.R124C), and c.1664G>A (p.R555W). All qPCR-positive results were verified by Sanger sequencing (Fig. 4b). Multidisciplinary consultations involving clinicians, genetic counselors, and surgeons were performed to evaluate the clinical status, genetic characteristics, and individual needs of each carrier. After comprehensive multidisciplinary evaluation and further communication with the subjects and their families, refractive surgery was ultimately cancelled for all six mutation-positive carriers and regular follow-up was scheduled.

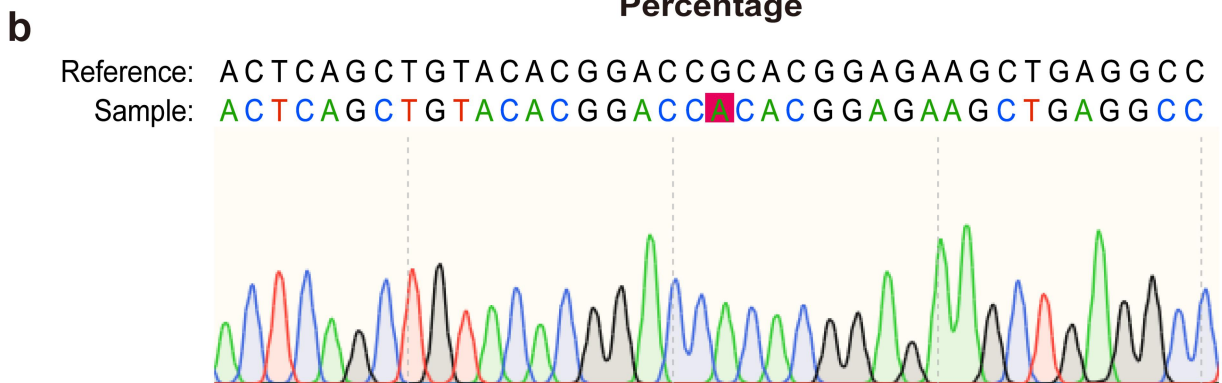
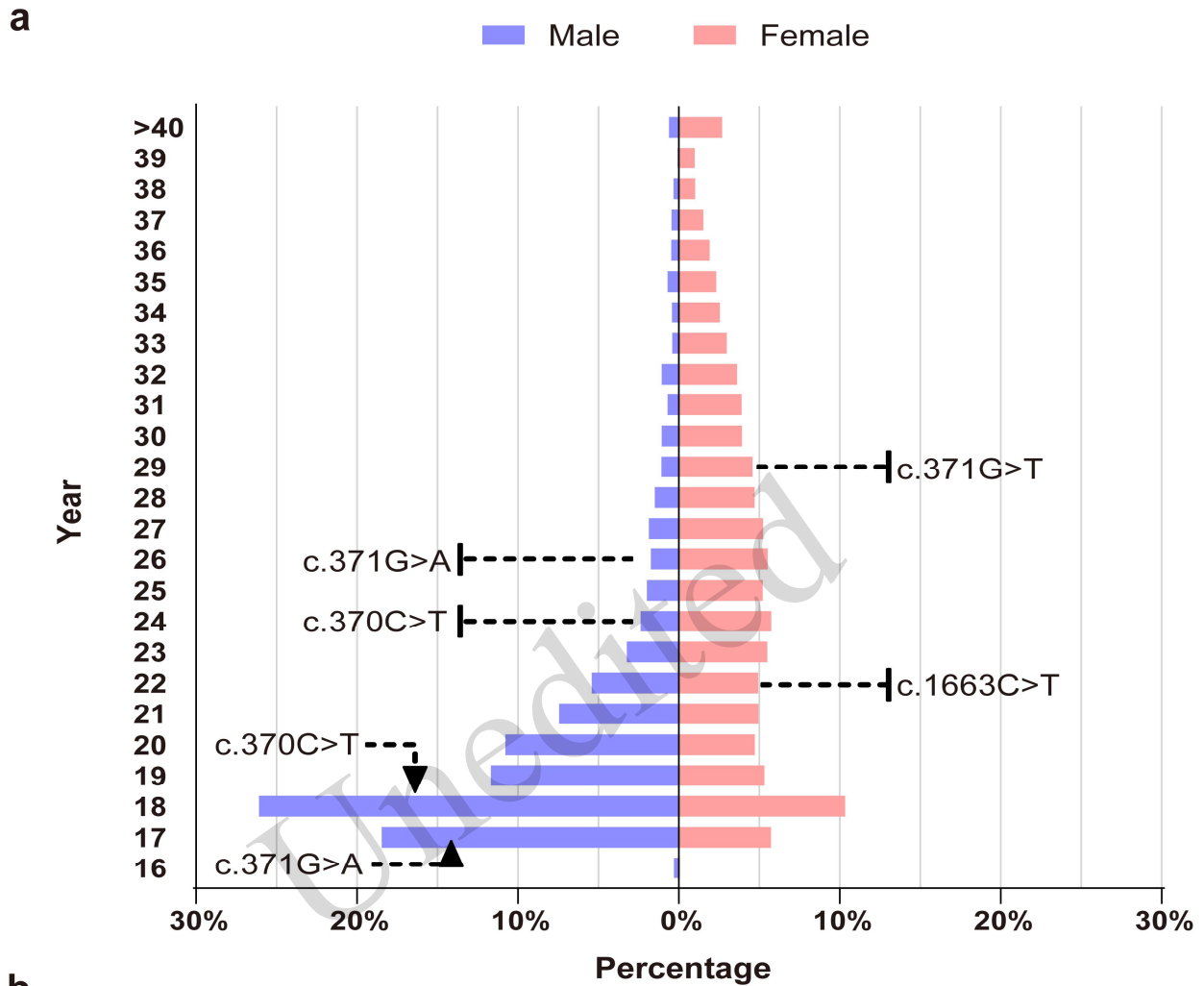


Fig. 4. Application of the validated multiplex quantitative polymerase chain reaction (qPCR) assay in a large preoperative screening cohort of 10,055 refractive surgery candidates. (a) Distribution and frequency of detected transforming growth factor beta-induced (*TGFBI*) hotspot mutations; (b) Sanger-sequencing confirmation of a qPCR-positive c. 371G>A homozygous sample.

4 Discussion

In this study, we developed a multiplex allele-specific qPCR assay targeting five recurrent *TGFBI* hotspot mutations and established an analytical validation framework to address a key unmet clinical need: reliable presurgical detection of asymptomatic carriers at risk for *TGFBI*-related corneal dystrophies. As outlined in the Introduction, slit-lamp examination alone is insufficient for identifying genetically predisposed individuals,

particularly young refractive surgery candidates. Against this background, a rapid, standardized, and statistically supported genetic screening method is essential for improving preoperative risk assessment (Wang et al.,2020).

The analytical strategy used here incorporates statistical modeling and experimental evaluation in a structured manner that aligns with contemporary analytical chemistry principles. The allele-calling thresholds are a result of ROC-based analyses, and the unified decision threshold is justified by clustering of locus-specific cutoffs. This threshold standardization is consistent with the assay's intended clinical application; it reduces interpretive variability while maintaining analytical rigor. Likewise, the quantitative estimates of detection limits are the outcome of Probit modeling of two-fold dilution data, and are supported by independent replicate testing. The agreement between modeled and empirical LOD values strengthens confidence in the assay's performance at low template concentrations, where precision is often most challenging (Banning et al.,2006). Results from precision, specificity, and interference studies further reinforce the robustness of the proposed assay. The low levels of intra- and inter-day variation, together with consistent performance across operators, reflect stable amplification behavior and reliable allele discrimination (Poulsen et al.,2016). These findings collectively confirm the assay's analytical stability under conditions representative of clinical laboratory workflows.

The large-scale administration of the assay to 10,055 refractive surgery candidates demonstrates its operational feasibility and provides a clinically relevant context for interpreting analytical metrics. The observed carrier rate of 0.06% in this study is slightly lower than the 0.1%–0.3% rate reported in other East Asian population-based studies. We attribute this discrepancy primarily to the unique characteristics of the study cohort: all participants were refractive surgery candidates recruited from a tertiary ophthalmic center, who underwent comprehensive preoperative ophthalmic assessment and generally presented with no clinically evident corneal pathology. Thus, the cohort represents a selected "healthier-cornea" subpopulation, rather than a random population-based sample. Additional factors contributing to the prevalence difference may include variations in recruitment settings, age structures, regional genetic characteristics, and the hotspot-targeted testing strategy used in this study. Therefore, the 0.06% prevalence estimate should be interpreted as the mutation rate in refractive surgery candidates, not the general East Asian population.

Although the mutation frequency we found was low (0.06%), the identification of both heterozygous and homozygous carriers underscores the importance of targeted genetic screening in populations that otherwise appear healthy. The complete concordance between qPCR and Sanger sequencing in all positive cases supports the validity of the assay as a primary screening tool. These observations are consistent with established epidemiological patterns of *TGFBI* dystrophies and reinforce the utility of hotspot-based assays for focused, high-throughput clinical screening (Zeng et al.,2017).

This multiplex qPCR platform offers distinct advantages compared with other *TGFBI* screening strategies, including full-gene Sanger sequencing and next-generation sequencing (NGS) panels. Full-gene Sanger sequencing (the gold standard for *TGFBI* genotyping) offers comprehensive mutation coverage but has limitations in large-scale screening due to its low throughput, long turnaround time, and high per-sample cost. NGS panels enable simultaneous detection of multiple mutations in multiple genes and provide broad mutation coverage, but they require complex experimental workflows, time-consuming data analysis, expensive instrumentation and reagents, and are not easily accessible for basic clinical laboratories. In contrast, our qPCR assay is a statistically validated, high-throughput tool designed specifically for preoperative screening, with the advantages of rapid turnaround, low cost, simple operation, and high scalability. It is not intended to replace comprehensive sequencing-based diagnostics, but to serve as an efficient first-tier screening method for large cohorts of refractive surgery candidates.

The core purpose of this screening strategy is to identify high-risk individuals with *TGFBI* gene mutations at an early stage, so as to intervene in advance and reduce the risk of adverse clinical outcomes. The clinical relevance of this assay is further highlighted by the standardized post-screening workflow implemented for positive results. qPCR-positive findings are first confirmed by Sanger sequencing, with the next steps being

evaluation by a corneal specialist and genetic counseling for affected individuals. Treating clinicians integrate genetic results with clinical findings to make individualized surgical decisions, including possibly cancelling surgery or modifying the surgical approach. This workflow ensures that genetic screening results are directly translated into clinical decision-making to reduce postoperative iatrogenic risk. In terms of cost-effectiveness, we quantified the total cost of large-scale screening (including sample collection, detection reagents, instrument operation, personnel training, and quality control) and considered economies of scale. Expanded screening volume is expected to reduce the unit cost of reagents and instrument depreciation, alleviating the program's overall economic burden. For benefit evaluation, we focused on reducing subsequent clinical treatment costs and improving patients' quality of life: early identification of positive subjects enables timely intervention, which prevents or delays disease progression, thus reducing medical expenses (e.g., corneal transplantation, opacity treatment, long-term medication) and medical resource burden. It also maintains visual function, avoiding irreversible visual impairment-related physical and psychological distress, and thus yielding significant intangible social and humanistic value. Clinically, the proposed assessment program fills the gap in early diagnosis of related genetic diseases, provides a basis for clinical decision-making, and helps formulate personalized management plans (e.g., regular follow-up for *TGFBI* carriers with normal slit-lamp results to monitor corneal lesions and improve prognosis). In terms of promotion, it is scalable and can be integrated into routine or specialized ophthalmic screening, especially for high-incidence regions and families with relevant genetic history, improving case-detection efficiency; it also enhances public awareness of genetic disease and preventive health care, laying a foundation for hierarchical disease prevention and control.

Some limitations should be acknowledged. First, the assay is only designed to detect the most common hotspot mutations and does not cover the full spectrum of rare or atypical pathogenic variants. Second, all samples were recruited from a single tertiary ophthalmic center, which may limit the generalizability of the results to other populations or clinical settings. Finally, the clinical consequences for mutation-positive individuals in the screened cohort were not evaluated longitudinally, and the predictive value of presurgical genetic screening on postoperative outcomes remains to be determined.

Despite these limitations, the present work provides a statistically grounded and experimentally validated platform for routine preoperative genetic assessment. By integrating ROC-guided cutoff selection, Probit-derived detection limits, and comprehensive analytical performance testing, this assay offers a reproducible and operationally simple approach for identifying *TGFBI* mutation carriers in large clinical populations. The methodology described here also provides a generalizable model for developing similar multiplex qPCR assays for other clinically actionable genetic markers, supporting broader efforts to incorporate quantitative molecular diagnostics into clinical decision-making.

5 Conclusions

This work establishes a multiplex allele-specific qPCR assay that enables rapid and standardized detection of five clinically significant *TGFBI* hotspot mutations. The assay's performance—defined by statistically calibrated Ct thresholds, experimentally verified detection limits, and stable precision across operators and conditions—demonstrates a high level of analytical robustness. Its successful application in more than 10,000 refractive surgery candidates highlights not only operational scalability but also the value of integrating quantitative molecular methods into routine presurgical evaluation.

Importantly, the analytical framework developed here provides more than a diagnostic tool: it introduces a reproducible, data-driven approach that supports precise, laboratory-ready decision thresholds and improves the reliability of genetic risk assessment. The standardized post-screening clinical workflow ensures that genetic results are effectively integrated into preoperative clinical decision-making, and the assay's cost-effective high-throughput design makes it suitable for large-scale clinical application. By offering a method capable of producing consistent, interpretable, and clinically actionable results, this study enhances the quality and precision of molecular testing in ophthalmic clinical laboratories and beyond.

Data availability statement

The dataset used or analyzed during the current study is available from the corresponding author on reasonable request.

Acknowledgments

The authors extend their sincere gratitude to the Refractive Surgery Center team at the Eye Hospital of Wenzhou Medical University for providing valuable data critical to the completion of this study. Their contribution was essential to the success of this research. This work was supported by the Wenzhou Science and Technology Plan Project (Grant No. ZY2022018).

Author contributions

Yunfeng Gu, Yi Xu, Xiaoling Li, and Meiqin Zheng conceived and designed the study. Shihao Chen, Yunfeng Gu, Liping Mao, Kangxuan Sun, and Qiuruo Jiang recruited the patients and collected the clinical data. Yi Xu, Yunfeng Gu and Xiaoling Li drafted the manuscript. Yi Xu, Yunfeng Gu, Wenhui Wu, and Yangyang Shen critically reviewed and revised the manuscript. All authors read and approved the final manuscript. All authors have read and agreed to the published version of the manuscript, and therefore, have full access to all the data in the study and take responsibility for the integrity and security of the data.

Compliance with ethics guidelines

Yunfeng Gu, Liping Mao, Xiaoling Li, Kangxuan Sun, Qiuruo Jiang, Wenhui Wu, Yangyang Shen, Shihao Chen, Meiqin Zheng, Yi Xu declare that they have no conflicts of interest.

All procedures followed were in accordance with the ethical standards of the responsible committee on human experimentation (institutional and national) and with the Helsinki Declaration of 1975, as revised in 2008 (5). Informed consent was obtained from all patients for being included in the study. Additional informed consent was obtained from all patients for whom identifying information is included in this article. The study protocol was approved by the Research Ethics Committee of Wenzhou Medical University (Approval Number: 2025-007-K007).

Declaration on the use of generative AI tools

No generative AI tools were used in the preparation of this manuscript.

References

- Banning CS, Kim WC, Randleman JB, et al., 2006. Exacerbation of Avellino corneal dystrophy after LASIK in North America. *Cornea*, 25(4): 482–484.
<https://doi.org/10.1097/01.icc.0000195949.93695.37>
- Bostan C, Randleman JB, 2024. Unilateral Granular Type 2 Corneal Dystrophy With Exacerbation After LASIK. *Cornea*, 43(5): 648–651.
<https://doi.org/10.1097/ICO.0000000000003490>
- Chao-Shern C, DeDionisio LA, Jang JH, et al., 2019. Evaluation of *TGFBI* corneal dystrophy and molecular diagnostic testing. *Eye*, 33: 874–881.
<https://doi.org/10.1038/s41433-019-0346-x>
- Cho EH, Lee M, Ki CS, et al., 2025. Genetic epidemiology of epithelial-stromal *TGFBI* dystrophies in a large Korean population. *Scientific Reports*, 15(1): 25360.
<https://doi.org/10.1038/s41598-025-08189-7>
- Gao JH, Liu K, Chen Z, 2021. IMI impact of myopia. *Chinese Journal of Experimental Ophthalmology*, 39(12): 1091–1103. (in Chinese).
<https://doi.org/10.3760/cma.j.cn115989-20210623-00369>
- Han KE, Choi SI, Kim TI, et al., 2016. Pathogenesis and treatments of *TGFBI* corneal dystrophies. *Progress in Retinal and Eye Research*, 50: 67–88.
<https://doi.org/10.1016/j.preteyeres.2015.11.002>
- Hieda O, Kobayashi A, Sotozono C, et al., 2023. Corneal Electrolysis for Granular Corneal Dystrophy Type 2 (Avellino Corneal Dystrophy) Exacerbation After LASIK. *Journal of Refractive Surgery*, 39(1): 61–65.
<https://doi.org/10.3928/1081597X-20221129-01>
- Holden BA, Fricke TR, Wilson DA, et al., 2016. Global prevalence of myopia and high myopia and temporal trends from 2000 through 2050. *Ophthalmology*, 123(5): 1036–1042
<https://doi.org/10.1016/j.ophtha.2016.01.006>
- Jiang X, Zhang H, 2021. Deterioration of Avellino corneal dystrophy in a Chinese family after LASIK. *International Journal of Ophthalmology*, 14(6): 795–799.
<https://doi.org/10.18240/ijo.2021.06.02>
- Kwak JJ, Yoon SH, Seo KY, et al., 2021. Exacerbation of Granular Corneal Dystrophy Type 2 After Small Incision Lenticule

- Extraction. *Cornea*, 40(4): 519–524.
<https://doi.org/10.1097/ICO.0000000000002655>
- Liskova P, Skalicka P, Dudakova L, et al., 2025. Genotype-phenotype correlations in corneal dystrophies: advances in molecular genetics and therapeutic insights. *Clinical and Experimental Ophthalmology*, 53(3): 232–245.
<https://doi.org/10.1111/ceo.14516>
- Li W, Qu N, Li JK, et al., 2021. Evaluation of the genetic variation spectrum related to corneal dystrophy in a large cohort. *Frontiers in Cell and Developmental Biology*, 9: 632946.
<https://doi.org/10.3389/fcell.2021.632946>
- Munier FL, Korvatska E, Djemaï A, et al., 1997. Kerato-epithelin mutations in four 5q31-linked corneal dystrophies. *Nature Genetics*, 15(3): 247–251.
<https://doi.org/10.1038/ng0397-247>
- Poulsen ET, Nielsen NS, Jensen MM, et al., 2016. LASIK surgery of granular corneal dystrophy type 2 patients leads to accumulation and differential proteolytic processing of *TGFBI*. *Proteomics*, 16(3): 539–543.
<https://doi.org/10.1002/pmic.201500287>
- Rocha-De-Lossada C, Rachwani-Anil R, Colmenero-Reina E et al., 2021. Laser refractive surgery in corneal dystrophies. *Journal of Cataract & Refractive Surgery*, 47(5): 662–670.
<https://doi.org/10.1097/j.jcrs.0000000000000468>
- Skonier J, Neubauer M, Madisen L, et al., 1992. cDNA cloning and sequence analysis of beta ig-h3, a novel gene induced after treatment with transforming growth factor-beta. *DNA and Cell Biology*, 11(7): 511–522.
<https://doi.org/10.1089/dna.1992.11.511>
- Song XD, Wu QY, Zhu PR, et al., 2023. Pathogenic mutation of *TGFBI* gene in a family with corneal dystrophy. *Clinical Laboratory Science*, 41(3): 176–179.(in Chinese).
<https://doi.org/10.13602/j.cnki.jcls.2023.03.04>
- Song Y, Sun M, Wang N, et al., 2017. Prevalence of transforming growth factor β -induced gene corneal dystrophies in Chinese refractive surgery candidates. *Journal of Cataract & Refractive Surgery*, 43: 1489–1494.
<https://doi.org/10.1016/j.jcrs.2017.07.038>
- Stenson, PD., Mort, M, Ball, EV, et al., 2020. The Human Gene Mutation Database (HGMD®): optimizing its use in a clinical diagnostic or research setting. *Human Genetics*, 139(10): 1197–1207.
<https://doi.org/10.1007/s00439-020-02199-3>
- Valasek MA, Repa JJ, 2005. The power of real-time PCR. *Advances in Physiology Education*, 29(3): 151–159.
<https://doi.org/10.1152/advan.00019.2005>
- Wang XR, Zhou BT, Zheng QM, et al., 2020. A recognition survey of granular corneal dystrophy type 2 genetic detection in China. *International Journal of Ophthalmology*, 13(12): 1976–1982.
<https://doi.org/10.18240/ijo.2020.12.20>
- Wang Y, Shi WY, Li Y, 2020. The rapid development and changes of corneal refractive surgery in China. *Chinese Journal of Ophthalmology*, 56(2): 81–85.(in Chinese).
<https://doi.org/10.3760/cma.j.issn.0412-4081.2020.02.001>
- Weiss JS, Rapuano CJ, Seitz B, et al., 2024. IC3D Classification of Corneal Dystrophies—Edition 3. *Cornea*, 43: 466–527.
<https://doi.org/10.1097/ico.0000000000003420>
- Zeng L, Zhao J, Chen Y, et al., 2017. *TGFBI* gene mutation analysis of clinically diagnosed granular corneal dystrophy patients prior to PTK: a pilot study from Eastern China. *Scientific Reports*, 7(1): 596.
<https://doi.org/10.1038/s41598-017-00716-5>
- Zhang FJ, Song YZ, 2023. Interpretation of the group standard “Technical specifications for laser corneal refractive surgery Part 1”. *Chinese Journal of Ophthalmology*, 59(6): 505–508.(in Chinese).
<https://doi.org/10.3760/cma.j.cn112142-20230117-00025>

Supplementary information:

Tables S1-S7; Figs. S1-S2;